

Online identification of internal impedance of Li-ion battery cell using ternary-sequence injection

Sihvo, Jussi ; Messo, Tuomas; Roinila, Tomi; Luhtala, Roni; Stroe, Daniel-Ioan

Published in:

Proceedings of the 2018 IEEE Energy Conversion Congress and Exposition (ECCE)

DOI (link to publication from Publisher):

[10.1109/ECCE.2018.8558147](https://doi.org/10.1109/ECCE.2018.8558147)

Publication date:

2018

Document Version

Accepted author manuscript, peer reviewed version

[Link to publication from Aalborg University](#)

Citation for published version (APA):

Sihvo, J., Messo, T., Roinila, T., Luhtala, R., & Stroe, D.-I. (2018). Online identification of internal impedance of Li-ion battery cell using ternary-sequence injection. In *Proceedings of the 2018 IEEE Energy Conversion Congress and Exposition (ECCE)* (pp. 2705-2711). IEEE Press. <https://doi.org/10.1109/ECCE.2018.8558147>

General rights

Copyright and moral rights for the publications made accessible in the public portal are retained by the authors and/or other copyright owners and it is a condition of accessing publications that users recognise and abide by the legal requirements associated with these rights.

- Users may download and print one copy of any publication from the public portal for the purpose of private study or research.
- You may not further distribute the material or use it for any profit-making activity or commercial gain
- You may freely distribute the URL identifying the publication in the public portal -

Take down policy

If you believe that this document breaches copyright please contact us at vbn@aub.aau.dk providing details, and we will remove access to the work immediately and investigate your claim.

Online identification of internal impedance of Li-ion battery cell using ternary-sequence injection

Jussi Sihvo

*Department of Electrical Energy Engineering
Tampere University of Technology
Tampere, Finland
jussi.sihvo@tut.fi*

Tuomas Messo

*Department of Electrical Energy Engineering
Tampere University of Technology
Tampere, Finland
tuomas.messo@tut.fi*

Tomi Roinila

*Department of Automation
Tampere University of Technology
Tampere, Finland
tomi.roinila@tut.fi*

Roni Luhtala

*Department of Automation
Tampere University of Technology
Tampere, Finland
roni.luhtala@tut.fi*

Daniel I. Stroe

*Department of Energy Technology
Aalborg University
Aalborg, Denmark
dis@et.aau.dk*

Abstract—The internal impedance of a battery has been shown to change as a function of state-of-charge (SOC) and state-of-health (SOH). Therefore, on-line impedance measurements can provide useful information for SOC- and SOH-estimation algorithms. Broad-band injections techniques such as pseudo-random-binary-sequence (PRBS) are attractive alternative for replacing conventional electrochemical-impedance-spectroscopy (EIS) which is very slow for online battery impedance measurements. However, non-linearities of batteries have a negative impact on the measurement results obtained by the PRBS for which the identified system is assumed to be linear. This paper demonstrates the use of ternary-sequence excitation signal for battery impedance measurements. Appropriately designed ternary-sequence can efficiently capture the linear component of the impedance by canceling out the distortion caused by the non-linear parts. The presented method can be used for rapid impedance measurements and thus, as a valuable tool in online SOC- and SOH-estimation algorithms. Experimental measurements are shown from a Lithium-Iron-Phosphate (LiFePO₄) battery cell.

Index Terms—Li-ion batteries, Internal impedance, on-line state estimation, PRBS, ternary-sequence, EIS

I. INTRODUCTION

The number of applications involving Li-ion batteries has rapidly increased in recent years. Especially the electric vehicles (EV) and energy storages have introduced a need for high power and energy applications involving Li-ion batteries. However, Li-ion batteries are more

unstable and unpredictable than other battery chemistries which tightens the requirements for the battery management system (BMS) [1].

Li-ion batteries are typically characterized by State-of-Charge (SOC) and State-of-Health (SOH). The SOC indicates the available charge that can be extracted from the battery. The SOH indicates the degradation of the battery and its capability to meet the requirements in the application. None of these parameters cannot be directly measured. Nevertheless, they can be estimated from other measurable quantities such as battery voltage, temperature, current and cycle life. Moreover, these quantities have non-linear dependency on the SOC and the SOH which complicates their accurate estimation. As the power levels and energy contents of the Li-ion batteries increase, the performance improvement of the BMS will be of great importance in future applications. [1]–[4]

As it was reported in the literature, the internal impedance of the batteries is changing with the SOC and can be used to predict the battery SOH [1], [2], [5]–[7]. Therefore, online internal impedance measurements can potentially be used for the SOC and SOH estimation in the BMS. In batteries, the internal impedance is usually determined using the Electrochemical Impedance Spectroscopy (EIS) where the battery is perturbed by sinusoidal excitation at different frequencies [1], [2], [6],

[8]. The method is, however, very slow and complex which makes it challenging to be implemented in online battery applications.

Alternative for conventional EIS is the use of broadband signals for the internal impedance online characterization. Particularly Pseudo-Random-Binary-Sequence (PRBS) excitations can significantly reduce the measurement complexity and time required for the measurements [5], [9], [10]. However, the highly non-linear behavior of batteries makes the internal impedance measurements with PRBS challenging because the perturbation is intended for identification of linear systems [11]. However, the effect of system non-linearities can be suppressed by designing a three-level ternary-sequence to more efficiently capture the linear part of the battery internal impedance spectrum [11]–[14].

An online battery internal impedance measurement method using a ternary-sequence excitation is proposed in this paper. The rest of the paper is organized as follows. The internal impedance of the battery and its dependency on the battery state parameters along with different measurement techniques are discussed in Section II. The non-linear system representation and the design of the ternary-sequence injection are discussed in Section III. The measurement setup and results are presented in Sections IV and V, while conclusions in Section VI.

II. INTERNAL IMPEDANCE OF THE BATTERY

Internal impedance of the battery is a parasitic feature that causes a voltage drop to the battery terminal voltage when current is drawn from the battery. It is also a frequency-dependent quantity which means that the voltage magnitude and phase shift to applied current is varying over different frequencies. The battery internal impedance $Z(j\omega)$ can be represented in the frequency domain as

$$Z(j\omega) = \frac{V(j\omega)}{I(j\omega)}, \quad (1)$$

where $V(j\omega)$ and $I(j\omega)$ are the Fourier-transformed voltage and current of the battery. Fig. 1 shows an example of LiFePO₄ battery internal impedance, where the characteristic parts of the internal impedance and the corresponding frequencies have been illustrated. At the simplest case, three regions with different characteristics can be observed depending on the battery SOC, chemistry and temperature. The Ohmic region is realized when the impedance curve crosses the real axis towards higher frequencies. The charge-transfer region is realized by capacitive behavior shaped as a semi-circle. At last,

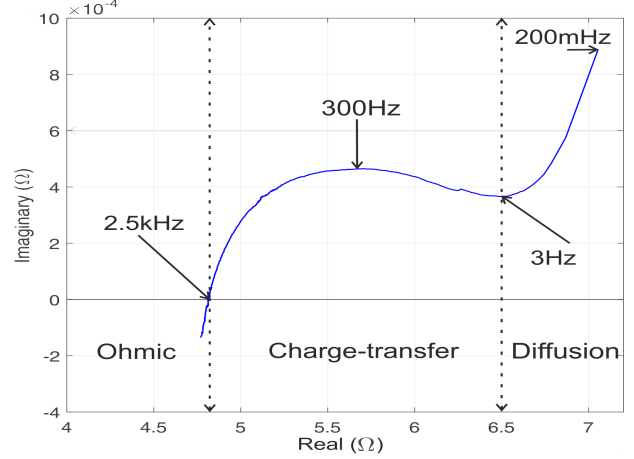


Fig. 1: An example battery internal impedance plot from real measurements with different regions and corresponding frequency points

the diffusion effect is realized at very low frequencies as a constant slope. [7]

The shape of the internal impedance has been shown to change as a function of SOC and SOH in different frequency regions [1], [2], [6]. For example for an LiFePO₄ battery cell, the dependency on SOC is taking place at low frequencies while SOH is normally analyzed at around few kilohertz where the impedance imaginary part is zero [1], [2]. Batteries are widely modeled by an equivalent-circuit-model (ECM) often regarded as Randles' model which is often used in SOC and SOH estimation algorithms [1], [3], [4]. Parameters of the ECM can be derived from the data of the complex impedance plot. However, it should be noted that the shape of the internal impedance highly depends on the battery chemistry and temperature. Therefore, online internal impedance measurements from very low to high frequencies with dense resolution could provide valuable information about the present battery state for the BMS.

A. Measurement techniques

The low magnitude of the internal impedance makes its measurements challenging. The internal impedance of the battery is conventionally analyzed by EIS which is also used for other electrochemical system identification [8], [15], [16]. In the EIS measurements, batteries are excited with a sinusoidal current which introduces a change in the terminal voltage from which the impedance is obtained according to (1). The EIS is, however, very slow because in the method, sinusoids with different frequencies are subsequently injected. This accumulates to a very long total measurement time which is unde-

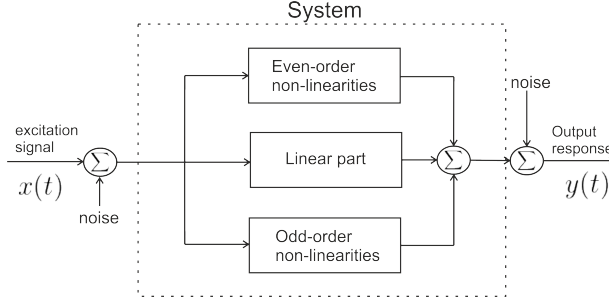


Fig. 2: Block diagram of non-linear systems

sired for online applications. Another problem with the conventional EIS is that it would be difficult to generate sinusoidal injections in practical applications.

A potential alternative to reduce the complexity of the system and the impedance measurement time is to use broadband signals like PRBS. The applicability of the PRBS for impedance measurements has been studied in [5], [9], [10]. The results obtained by the PRBS are, however, affected by the non-linear behavior of the battery and are suffering from poor accuracy. To reduce the effect of the non-linearities, more sophisticated perturbation signal should be used.

III. NON-LINEAR SYSTEM IDENTIFICATION USING EXTERNAL INJECTION

Non-linear systems can be represented by linear part along with even- and odd-order non-linear parts. A principal scheme of such concept is illustrated in Fig. 2, where $x(t)$ denotes the system input and $y(t)$ is the system output. Along with noise in system's input and output measurements, system's linear and non-linear dynamics are always present. The dynamics of the linear part are often the desired content to be measured from a system, and, therefore, the aim is to suppress the effect of non-linear dynamics [11]–[13].

A. Ternary-sequence

Ternary-sequences are broadband signals which have three signal levels and similar frequency- and time-domain characteristics as the well-known two-level PRBS perturbation signals [11]. However, the ternarity of the signal allows to design the sequence in a way that even-order and some odd-order harmonics can be suppressed in the sequence frequency spectrum. Ternary-sequences also exists for greater number of possible signal lengths than PRBS which gives more freedom to design the practical implementation. In this paper, a ternary-sequence with suppressed even-order harmonics

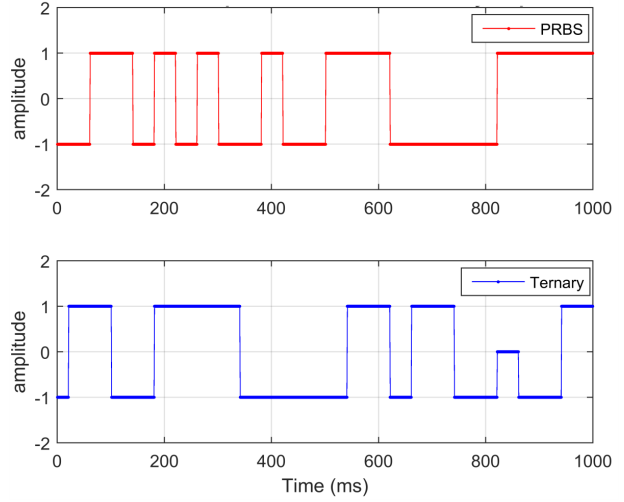


Fig. 3: Time-domain responses of PRBS and ternary-sequence

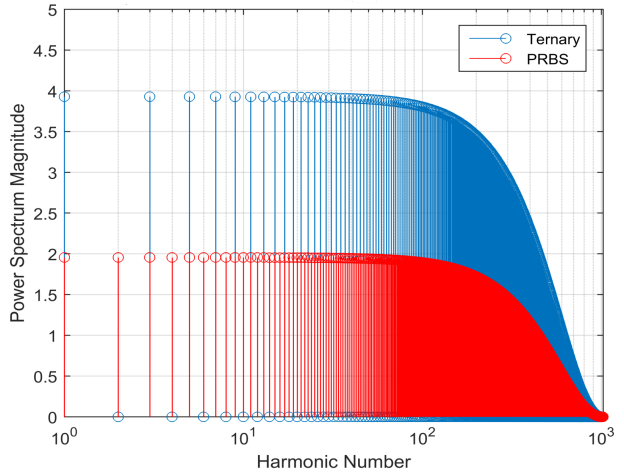


Fig. 4: Frequency-domain responses of PRBS and ternary-sequence

is applied. The synthesis of such and other types of ternary sequences are documented in [12], [13].

The ternary-sequence and PRBS are compared in Figs. 3 and 4 in time- and frequency-domain with signal lengths of 1023 for the PRBS and 1018 for the ternary-sequence. Cancellation of even-order harmonics is illustrated in Fig. 4 where the ternary-sequence has zero power at even-order harmonic components. The non-zero components are strengthened to have twice the power compared to the PRBS. This feature allows the ternary-sequence to be designed with lower amplitude which is often a crucial limitation in real applications.

B. Perturbation design

The applied perturbation should have a bandwidth high enough to capture the beginning of the ohmic region of the impedance shown in Fig. 1. The highest frequency to be measured is theoretically determined by the generation frequency f_{gen} of the injection. Due to the decreasing power of the high frequency components, the bandwidth is restricted to approximately half of the f_{gen} in reality. The lowest frequency, that is, the frequency resolution f_{res} , is determined by the f_{gen} and the length of the sequence N by the relation

$$f_{res} = \frac{f_{gen}}{N} \quad (2)$$

which should be low enough to reliably capture the diffusion part. Due to the interest in low- and high frequency response of the internal impedance, very large N is required because the frequency points are linearly distributed between f_{res} and f_{gen} . This increases the amount of data to be stored for frequency response analysis. The amount of data can be reduced by using separate injections with different f_{res} excited subsequently as is done in [10]. Besides f_{res} and f_{gen} , another important parameter is the sampling frequency f_s which should be high enough to reduce the effect of sampling delay in the measurements.

The low magnitude of the battery internal impedance requires a relatively high amplitude for the injection to provide appropriate signal-to-noise-ratio (SNR). However, the amplitude should be small enough to keep the battery SOC at steady-state. A decent design guide for the selection of the amplitude is to compare the amplitude to the C-rate of the battery and not let the amplitude exceed the current of 1C.

C. Data smoothing with MAF

The measured data can be smoothened by moving-average-filter (MAF) to reduce to measurement time. Wider window in MAF smoothenes the deviation in the data more efficiently but introduces a greater delay to the smoothened data which is a half the length of the window in samples [17]. For battery impedance data smoothing, the MAF delay slightly distorts the low-frequency data. However, the high and medium frequencies are smoothened accurately.

IV. EXPERIMENTS

The experiments were carried out for lithium-iron-phosphate (LiFePO4) battery cell with nominal voltage of 3.3V and capacity of 2.3Ah at 35°C. To provide a

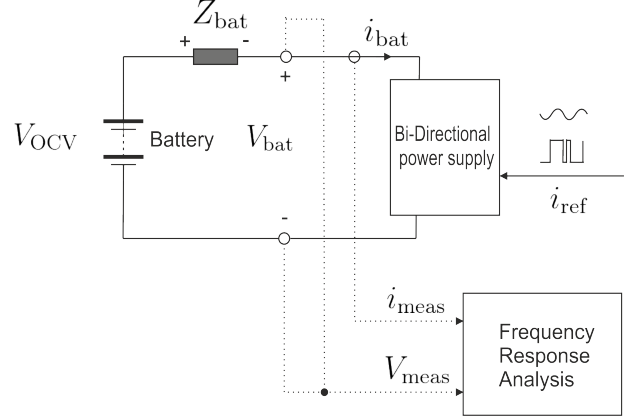


Fig. 5: Principal scheme of the battery impedance measurement setup

reliable reference, the measurements were also carried out with EIS analyzer.

The measurement scheme is shown in Fig. 5 and the actual measurement setup is shown in Fig. 6. The ternary-sequence and the PRBS are given as a reference for the bi-directional power supply to charge and discharge the battery. Discrete fourier-transform is applied to compute the impedance spectrum from the current- and voltage measurements. The SOC was monitored by Coulomb counting method [1] to illustrate the change in battery internal impedance within one discharge cycle. The battery impedance was measured with the PRBS and ternary sequence techniques at SOC's between 90% and 10%, considering 10% SOC resolution. In order to reach each desired SOC, the battery was discharged with a current of 1C. Then the battery was left to a rest at open-circuit for 30 minutes to reach the equilibrium

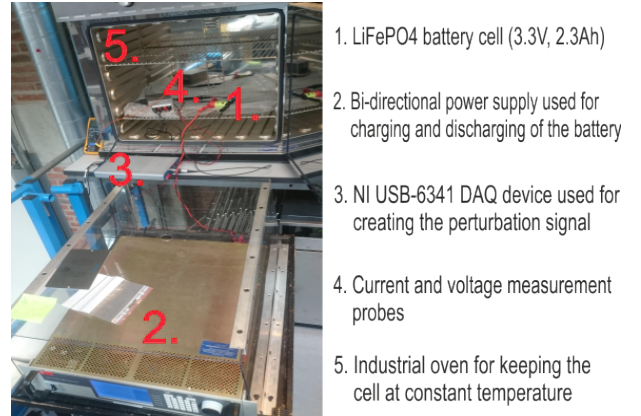


Fig. 6: Laboratory setup of the battery impedance measurements with device explanations

	EIS	PRBS	Ternary
Amplitude ($0 - p$)	$0.7A - 2A$	$1.15A$	$1.15A$
Averaging (P)	3	1	1
Frequency band	$10mHz - 6.4kHz$	$220mHz - 3.5kHz$	$220mHz - 3.5kHz$
f_{gen}	-	$7kHz$	$7kHz$
f_s	-	$175kHz$	$175kHz$
N	-	32767	32762
Measurement time	22min	4.7s	4.7s

TABLE I: Injection parameters for measurements

potential before the next measurement sweep. The measurements were carried out in stand-by mode meaning that the battery was both charged and discharged during the measurements. This was due to the limitations of carrying out measurements during charge/discharge with the EIS analyzer.

For the measurements applied in this paper, the generation frequency f_{gen} was set to 7 kHz for both the ternary and PRBS injections, providing impedance measurements up to 3.5 kHz. The signal lengths of 32762 for the ternary-sequence and 32767 for the PRBS were chosen to keep the signals as similar as possible. According to (2), this yields to frequency resolution of $\approx 220mHz$ which is low enough to capture the diffusion part of the internal impedance for the used battery cell. The amplitudes for both PRBS and ternary-sequence was selected as $1.15A$ which corresponds to C-rate of $0.5C$. A MAF with a window length of 30 datapoints was applied to the measurement results. The ternary-sequence was generated by using **prs** MATLAB-software provided in [12]. The parameters for the PRBS, ternary-sequence and EIS are all shown in Table I.

V. RESULTS

The impedance measurement results from a LiFePO4 battery cell are shown in Figs. 8 - 12. By comparing the results obtained by the ternary-sequence and the PRBS to the EIS reference measurements in Figs. 9 - 12, the superiority of the ternary-sequence over the PRBS can be well concluded. The impedance plot of the PRBS is slightly shifted to the right which means that it is experiencing additional resistance which is not present in the results produced by the ternary-sequence. The distorted results of the PRBS are even more visible in the frequency-domain which is illustrated in Fig. 7 at 40% of SOC. From 10Hz down to lower frequencies, the results produced by the PRBS are experiencing significant phase shift and also increased magnitude. This is most likely caused by the non-linear effects in the battery internal impedance. The effect of increased amplitude in the ternary-sequence harmonic components can be seen in Fig. 8 where both ternary-sequence and PRBS are shown before the MAF is applied. The results obtained by

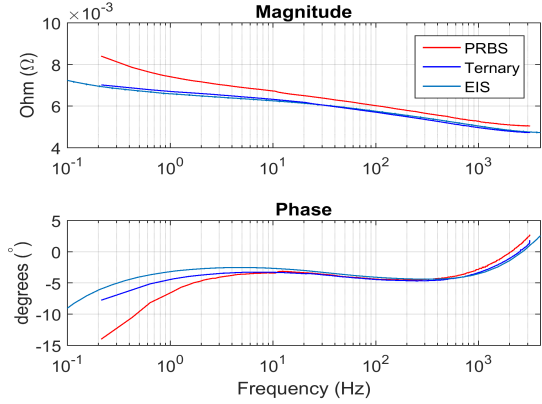


Fig. 7: Frequency response representation of the measured impedance at 40% SOC

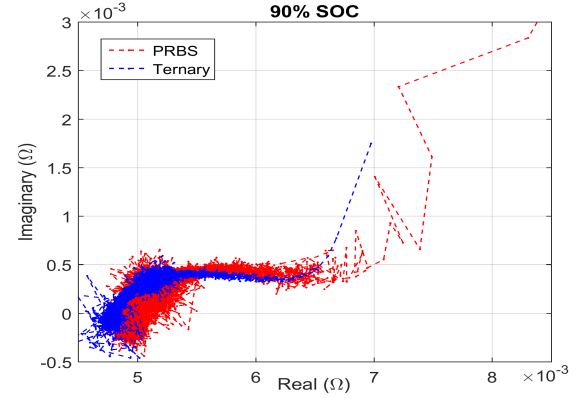


Fig. 8: Complex internal impedance plot at 90% SOC before MAF

the ternary sequence have quite consistent shape even before the MAF averaging while the results produced by the PRBS have huge deviation throughout the measured frequency band.

It can be seen that the results obtained by the ternary sequence are matching quite well to the EIS at every SOC value. Especially the high-frequency response in the ohmic region, and partly in the charge-transfer region, is captured very reliably. This includes also the zero-imaginary point in the battery impedance. Therefore, the ternary-sequence could be used reliably to SOH estimation in the BMS. The impedance spectrum corresponding to the charge-transfer region towards the diffusion region, is slightly different from the reference impedance spectrum obtained by EIS. The delay introduced by the MAF is considered to have a small impact in the diffusion region. However, the differences are most likely to be caused by the measurement setup. The setup

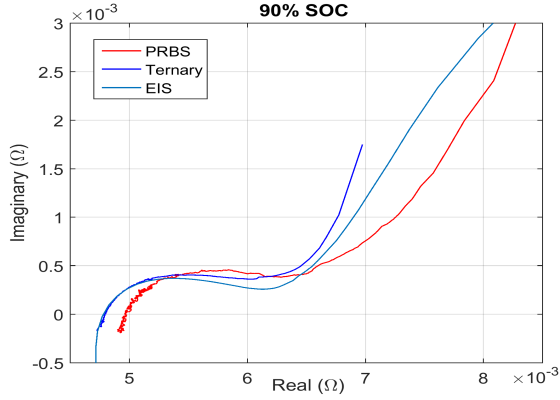


Fig. 9: Complex internal impedance plot at 90% SOC obtained with different measurement techniques

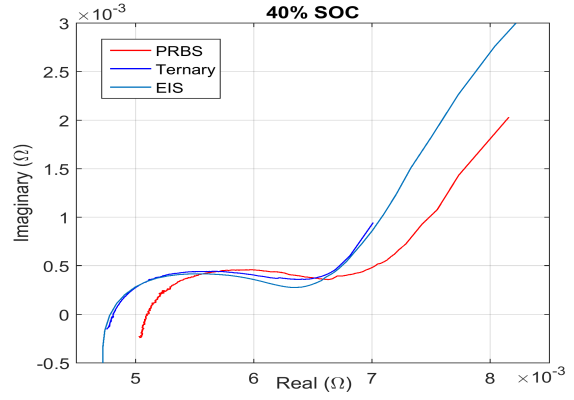


Fig. 11: Complex internal impedance plot at 40% SOC obtained with different measurement techniques

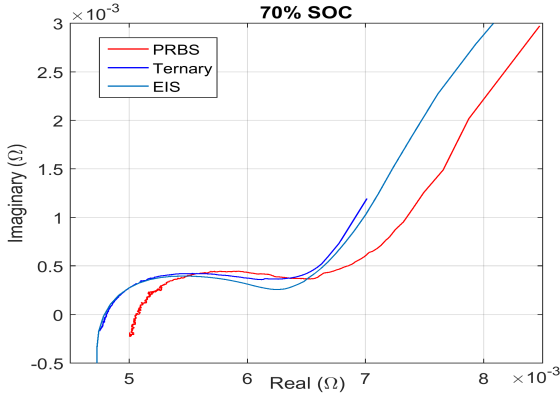


Fig. 10: Complex internal impedance plot at 70% SOC obtained with different measurement techniques

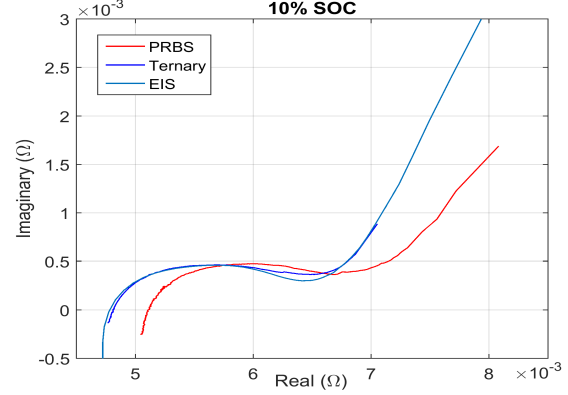


Fig. 12: Complex internal impedance plot at 10% SOC obtained with different measurement techniques

and measurement circuit in EIS analyzer is expected to be slightly different than the implemented setup. Due to the low magnitude of the internal impedance, even very small parasitic impedance in the measurement circuit are affecting the results. In order to make more relevant comparison, the EIS measurements should have been carried out with the implemented ternary-sequence setup. This, however, is challenging to implement using the existing hardware and is considered as a topic for further research. For batteries with higher internal impedance, the ternary-sequence is expected to have higher performance due to the reduced effect of the setup parasitic impedance.

Compared to the EIS measurements, the measurement time using the ternary-sequence and PRBS for each sweep was significantly faster. Each sweep took 4.8 seconds while a sweep with the EIS took over 20

minutes. In reality, the difference is smaller because the EIS measurements were carried out with three averaged periods while only one was used for the PRBS and ternary-sequence.

VI. CONCLUSIONS

This paper demonstrated an online identification technique for accurate and rapid measurement of the internal impedance of a battery. A ternary-sequence injection was applied, and the internal impedance was measured for a LiFePO₄ battery cell. The results were compared to results obtained by a conventional PRBS and also to reference data obtained by an EIS analyzer. Practical measurements showed that the ternary-sequence good resiliency to non-linear effects of the battery makes the measurement results more accurate compared to the conventional PRBS. The ternary-sequence also matches well to the reference results produced by the EIS while the

measurement time is significantly reduced. Considering also the low complexity of the ternary-sequence, the presented method is well suited for the SOC and SOH estimation in online applications of battery management systems.

REFERENCES

- [1] P. Weicker, *A Systems Approach to Lithium-Ion Battery Management*. Norwood, UNITED STATES: Artech House.
- [2] D. I. Stroe, M. Swierczynski, a. I. Stan, V. Knap, R. Teodorescu, and S. J. Andreassen, "Diagnosis of lithium-ion batteries state-of-health based on electrochemical impedance spectroscopy technique," *Energy Conversion Congress and Exposition (ECCE), 2014 IEEE*, pp. 4576–4582, 2014.
- [3] J. Meng, M. Ricco, G. Luo, M. Swierczynski, D. I. Stroe, A.-I. Stroe, and R. Teodorescu, "An Overview and Comparison of Online Implementable SOC Estimation Methods for Lithium-ion Battery," *IEEE Transactions on Industry Applications*, vol. 54, no. 2, pp. 1–1, 2017. [Online]. Available: <http://ieeexplore.ieee.org/document/8114258/>
- [4] M. Bercibar, I. Gandiaga, I. Villarreal, N. Omar, J. V. Mierlo, and P. V. D. Bossche, "Critical review of state of health estimation methods of Li-ion batteries for real applications," vol. 56, pp. 572–587, 2016.
- [5] S. Nejad, D. T. Gladwin, and D. A. Stone, "A hybrid battery parameter identification concept for lithium-ion energy storage applications," *IECON Proceedings (Industrial Electronics Conference)*, pp. 1980–1985, 2016.
- [6] A. Zenati, P. Desprez, and H. Razik, "Estimation of the SOC and the SOH of Li-ion batteries, by combining impedance measurements with the fuzzy logic inference," *IECON Proceedings (Industrial Electronics Conference)*, pp. 1773–1778, 2010.
- [7] C. R. Birkel and D. A. Howey, "Model identification and parameter estimation for LiFePO₄," *1st Catapult Conference: Energy Storage Technology*, pp. 1–6, 2013.
- [8] E. Karden, S. Buller, and R. W. De Doncker, "A method for measurement and interpretation of impedance spectra for industrial batteries," *Journal of Power Sources*, vol. 85, no. 1, pp. 72–78, 2000.
- [9] R. Al Nazer, V. Cattin, P. Granjon, M. Montaru, M. Ranieri, and V. Heiries, "Classical EIS and square pattern signals comparison based on a well-known reference impedance," *World Electric Vehicle Journal*, vol. 6, no. 3, pp. 800–806, 2013.
- [10] J. Sihvo, T. Messo, T. Roinila, and R. Luhtala, "Online Internal Impedance Measurements of Li-ion Battery Using PRBS Broad-band Excitation and Fourier Techniques : Methods and Injection Design," vol. 0, no. 1, 2018, pp. 2470–2475.
- [11] K. Godfrey, *Perturbation Signals for System Identification*, 1994.
- [12] A. H. Tan and K. R. Godfrey, "The generation of binary and near-binary pseudorandom signals: An overview," *IEEE Transactions on Instrumentation and Measurement*, no. 4, pp. 583–588.
- [13] K. Godfrey, H. Barker, and A. Tan, "Ternary input signal design for system identification," *IET Control Theory & Applications*, no. 5, pp. 1224–1233, sep.
- [14] T. Roinila and T. Messo, "Online Grid-Impedance Measurement Using Ternary-Sequence Injection," *IEEE Transactions on Industry Applications*, vol. 9994, no. c, 2018.
- [15] X. Wei, X. Wang, and H. Dai, "Practical On-Board Measurement of Lithium Ion Battery Impedance Based on Distributed Voltage and Current Sampling," *Energies*, vol. 11, no. 1, p. 64, jan 2018. [Online]. Available: <http://www.mdpi.com/1996-1073/11/1/64>
- [16] S. Moore and P. Barendse, "Online Condition Monitoring of Lithium-Ion Batteries Using Impedance Spectroscopy," pp. 5617–5624, 2017.
- [17] S. Golestan, M. Ramezani, J. M. Guerrero, F. D. Freijedo, and M. Monfared, "Moving average filter based phase-locked loops: Performance analysis and design guidelines," *IEEE Transactions on Power Electronics*, vol. 29, no. 6, pp. 2750–2763, 2014.